Int. J. Electrochem. Sci., 12 **(2017)** 6068 – 6080, doi: 10.20964/2017.07.14

International Journal of
ELECTROCHEMICAL
SCIENCE
www.electrochemsci.org

Improved Cycling Stability of Three-state Electrochromic Devices with Uniformly Dip-coated Electrode Surface

L. Wu, D.J. Yang, C.J. Hu, S. Liu, Q.G. Chen, J.Y. Shi, F. Wu, Y. Xiang[*]

School of Energy Science and Engineering, University of Electronic Science and Technology of China, 2006 Xiyuan Ave, West High-Tech Zone, Chengdu, Sichuan 611731, China.
[*]E-mail: xyg@uestc.edu.cn

Received: 20 February 2017 / *Accepted:* 16 April 2017 / *Published:* 12 June 2017

The electrodeposition-based three-state electrochromic device with its electrode surface modified by dip-coated titanium dioxide (TiO_2) thin films shows significantly improved cycling stability compared to the device modified with spin-coated ones. The decrement rate of optical transmittance contrast for spin-coated device after 1500 cycles is reduced significantly from 66% to 28% for dip-coated device, indicating ~60% improvement. A comparative study of the structural and morphological features of dip- and spin-coated TiO_2 thin films reveals that the surface uniformity of dip-coated device is much better than that of spin-coated one, leading to an improved overall surface roughness, which is a primary factor of the cycling stability. Although the difference in the surface roughness is marginal for the smooth parts of both the dip- and spin-coated TiO_2 thin films, the improved uniformity of the dip-coated TiO_2 thin film surface is conducive to the quick dissolution of Ag back into electrolyte during the switching between the coloration and bleaching states thanks to the reduced locally residual Ag around or into the rough regions caused by TiO_2 nanoparticles agglomeration.

Keywords: Electrodeposition; Electrochromic; Dip-coating; Uniformity; Cycling stability

1. INTRODUCTION

Electrochromic materials have the ability to reversibly change their optical properties when subjected to an electrical voltage. The pioneering work on the electrochromism dates back to 1969 when Deb developed the first tungsten trioxide based electrochromic device [1]. Since then, numerous attentions have been paid on electrochromism for various applications in smart windows, antiglare rear view mirrors, electrochromic displays, military camouflage, etc [2-8]. Electrochromic materials usually are classified into several categories, namely, transition metal oxides [9, 10], Prussian blue [11, 12], conducting polymers [13, 14], viologens [15, 16], transition metal ions coordination compound

[17, 18], hybrid electrochromic materials [19, 20], and reversible electrodeposition-based electrochromic materials [21-28]. Electrochromic devices based on reversible electrodeposition have simple sandwich-type structures, with electrolytes and electrodeposition components interspersed between two transparent conducting electrodes. The optical properties are manipulated via deposition of metal (copper, bismuth, plumbum, silver, etc.) onto transparent conducting electrodes under an applied voltage and dissolution of metal into the electrolyte upon removal of the voltage [21-27].

Usually, appropriate electrode surface modification may trigger multiple states of the electrodeposition-based electrochromic device due to the absorption and/or multiple scattering of light of the modified electrode surface [28-31]. Various techniques, including sputtering [32], vacuum evaporation [33], chemical vapour deposition [34], electrodeposition [35], and sol-gel [36, 37], can be utilized to deposit thin films on the surface of electrodes. Among various techniques, the sol-gel approach is advantageous due to its low cost, amenable for large area preparation and easy to handle properties, out of which the spin-coating and dip-coating techniques are widely used. Spin-coating technique are widely used to modify indium tin oxide (ITO) and TiO_2 nanoparticles onto transparent conductive electrodes to fabricate electrodeposition-based multiple-state electrochromic device [28-31]. Araki et al. [28] deposited Ag onto an indium tin oxide (ITO) electrode, the surface of which was modified by ITO nanoparticles using spin-coating technique, and obtained a reversible three-state device. Further pursuit of multiple coloration states has also been attempted by Tsuboi et al. [29, 30] through controlling the size of Ag grains using different voltages. In a previous study, our group fabricated an electrodeposition-based Ag/Cu electrochromic device with reversible three-state optical transformation using fluorine doped tin oxide (FTO) electrodes spin-coated with TiO_2 nanoparticles [31]. Compared with spin-coating technique, dip-coating technique is preferred due to its higher controllability, lower cost, and more applicable to large scale preparation. However, the dip-coating technique has not yet been applied in the fabrication of electrodeposition-based Ag/Cu electrochromic devices.

Device cycling stability, as one of the most important electrochromic properties, is strongly influenced by the transparent electrode surface morphology before and after repeatedly switching between its coloration and bleached states for a certain number of times. To the best of our knowledge, there have been few reports focusing on the effect of electrode surface morphology on the cycling stability of electrodeposition-based electrochromic device with multi-state optical transformation. The transparent electrode surface morphology is, furthermore, manipulated by the film preparation method [38, 39]. Basically, dip-coating technique is preferred due to its higher controllability and more applicable to large scale preparation compared with spin-coating [39]. Moreover, Deepa etc. [39] reported that dip-coated electrochromic devices based on tungsten trioxide (WO_3) thin films showed superior performance compared with spin-coated devices, such as improved transmission modulation, coloration efficiency, switching speed and coloration-bleached cycles. They demonstrated that the varied thin film structure and surface morphology, such as optimal porosity and grain size hints for dip-coating technique mainly attribute to the improved electrochromic properties. Therefore, the investigation of electrochromic properties of device with multiple states using dip-coated electrode is significant and challengeable.

In this study, we firstly applied the dip-coating technique to modify FTO electrodes with TiO_2 nanoparticles in electrodeposition-based electrochromic devices, achieving reversible three-state optical transformation between transparent, mirror, and black, with improved stability. When a suitable voltage applied, Ag in the gel electrolyte is deposited onto the flat FTO electrode or the opposite rough FTO electrode modified by TiO_2 nanoparticles depending on the polarity of the applied voltage, thus allowing the electrochromic device to change its optical states from transparent to mirror or black state. Reversely, Ag is dissolved into the gel electrolyte once the voltage is removed and the device changes back to the transparent state. The decrement rate of optical transmittance contrast for spin-coated device after 1500 cycles is reduced significantly from 66% to 28% for dip-coated device, indicating ~60% improvement in cycling stability. Transmittance below 1% in the black state and reflectance over 70% in the mirror state are obtained, with optical transmittance contrast of 50.1% and 35.7% after first and 1500 switching among three optical states controlled by sequential voltages measured, respectively. An electrodeposition-based electrochromic device was also fabricated by modifying the electrode surface using spin-coating for comparative study. The correlation between the device cycling stability and the modified electrode structure and surface morphology were investigated.

2. EXPERIMENTAL

2.1 Materials

FTO glass with size of 25×30 mm and with sheet resistance of 10 Ωsq^{-1} was used as the electrode and purchased from Wuhan Lattice Solar Energy Technology Co. Ltd. Uniform TiO_2 nanoparticles with average diameters of 5~10 nm (Aladdin Co. Ltd) were used to modify the FTO electrode. Electrolytes compounds including Dimethyl sulfoxide (DMSO, ≥99.8%, J&K Chemical Co. Ltd.), tetra-n-butylammoniumbromide (TBABr, ≥99%, J&K Chemical Co. Ltd.), silver nitrate ($AgNO_3$, ≥99.8%, Guangdong Guanghua Sci-Tech Co. Ltd.), copper chloride ($CuCl_2$, ≥99.0%, KeLong Chemical Co. Ltd.), poly (vinyl butyral) (PVB, Sekisui Chemical Co. Ltd.), ethyl cellulose (≥99.5%, HanzhouLanbo Industrial Co. Ltd.), lauric acid (≥99.8%, KeLong Chemical Co. Ltd.), terpineol (≥98.0%, KeLong Chemical Co. Ltd.) and ethyl alcohol (≥99.7%, KeLong Chemical Co. Ltd.) were obtained from commercial sources. All solvents and chemicals were of reagent quality and were used without further purification. Teflon sheets with a thickness of 0.5 mm were purchased from Aladdin Co. Ltd.

2.2 Preparation of TiO_2 nanoparticles dispersion and gel electrolyte

TiO_2 nanoparticles slurry was obtained by milling TiO_2 nanoparticles (2.5 g) mixed with lauric acid (0.25 g), ethyl cellulose (0.75 g), terpineol (16 mL) and ethyl alcohol (10 mL) for 50 min, followed by diluting the slurry with ethyl alcohol. To prepare the electrolyte, TBABr (806 mg),

$AgNO_3$ (85 mg), and $CuCl_2$ (13 mg) were dissolved in 10 mL of DMSO, followed by the addition of PVB (1.32 g).

2.3 Modification of FTO electrode and fabrication of electrochromic devices

10 ml ethyl alcohol was added to 5 mL TiO_2 nanoparticle dispersion, and ultrasonically mixed for 30 min. After that, FTO was fixed onto the dip-coater, immersed into the aforementioned dispersion, and lifted with a speed of 3000 □m/s. In addition, FTO was also fixed onto the spin-coater, 0.25 ml of the aforementioned dispersion was spin-coated onto the surface of the FTO electrode with a speed of 500 rpm for 5 s and 1500 rpm for 15 s subsequently, by which the same thickness of the spin-coated TiO_2 thin film as dip-coated one was achieved. Both the dip-coated and spin-coated samples were subsequently sintered for 30 min at 500 ℃. To assemble the electrodeposition-based electrochromic device, the DMSO-based gel electrolyte was contained in a hermetic square space of 20 mm × 20 mm, cut inside a Teflon sheet of 0.5 mm thickness, and sealed by sandwiching the Teflon sheet between two FTO electrodes, one of which was modified with TiO_2 nanoparticles.

2.4 Characterization

The morphology of TiO_2 nanoparticles modified FTO electrodes were characterized using a field-emission scanning electron microscope (FE-SEM, S-3400, Hitachi). The crystal structures of the films were examined by a glancing incidence X-ray diffraction (XRD) system (DX-1000, Dandong Haoyun Instrument Co. Ltd.). The roughness of TiO_2 nanoparticles modified FTO electrodes were characterized by using an atomic force microscope (AFM, Multimode V, Veeco). Electrochemical tests were conducted by using an electrochemical workstation (CHI660D, CHI). The transformation voltage was applied to the electrochromic devices using the electrochemical workstation (CHI660D, CHI), and the transmittance and reflectance spectra were measured using a UV-Vis spectrophotometer (Cary 5000, Agilent).

3. RESULTS AND DISCUSSION

3.1 Realizing reversible three-state optical transformation for voltage-controlled electrochromic device

By applying suitable voltages, the dip-coated electrochromic device exhibits three reversible optical states, including transparent, mirror, and black, as illustrated in Figure 1. The essential mechanism of transformed optical states is Ag deposition onto transparent conducting electrodes and dissolution into the electrolyte according to previous reports [28-31, 40-43]. Without applying voltage, the device is transparent, as the background letters UESTC can be seen clearly (Figure 1a and 1b). When a positive voltage (+2.5 V) is applied to the modified FTO electrode, the device turns into the mirror state with the deposition of Ag onto the unmodified FTO electrode (flat surface), as proved by

the reflection image of the red pen in Figure 1c and 1d. Similarly, the black state is obtained by applying a negative voltage (-2.5 V) to the modified FTO electrode (rough surface), as shown in Figure 1e and 1f. Thus it can be seen that the dip-coated electrodeposition-based electrochromic device can realize the same voltage controlled three-state optical transformation as previous reported Ag-based reversible electrochromic devices [28-31, 40-43].

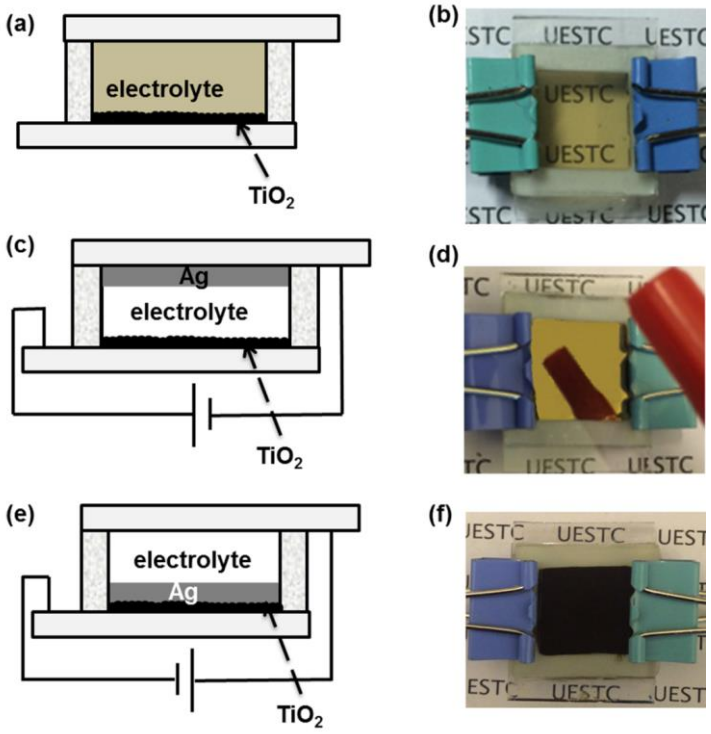

Figure 1. Schematic illustration and photographs showing the electrodeposition-based electrochromic devices in three different optical states: transparent state (a, b); mirror state (c, d); black state (e, f).

3.2 Investigation on the optical properties of dip-coated electrochromic device

To further confirm the effectiveness of dip-coating technique, transmittance and reflectance spectra of the dip-coated device were measured in the spectrum range of 400 nm~800 nm [31, 42]. For transmittance and reflectance measurement, voltages of +2.5 V and -2.5 V are applied to the TiO_2 nanoparticle-modified FTO electrode to obtain the mirror and black states, respectively. For transmittance measurement, the transmittance for device in transparent state is measured approximately 63% at 700 nm (Figure 2a). When applied with a negative voltage, the Ag is deposited onto the modified FTO electrode, leading to the device changes its optical state from transparent to black state, the transmittance drops to 13% quickly. The low transmittance appears to be comparable to the cell transmittance observed for ITO nanoparticles spin-coated device in coloration states [28]. The optical contrast, which is defined as the maximal difference of transmittance for electrochromic device between its coloration and bleaching processes, is measured to be 50.1%, which is as high as that reported by He et. al [44]. After trigger the mirror state by applying a positive voltage, decrease in

transmittance for device is also observed [42-44], as illustrated in Figure 2a. For reflectance measurement (Figure 2b), the reflectance for device in transparent and black states are below 30% (Figure 2b). The device in mirror state exhibits reflectance over 70%, as expected (Figure 2b). The obtained high reflectance is in good agreement with literature data [45].

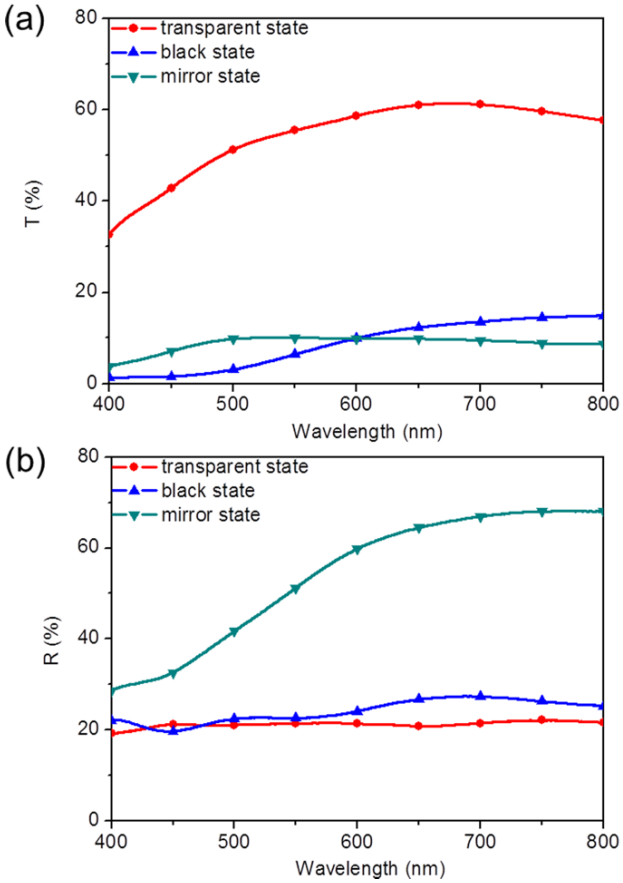

Figure 2. (a) Transmittance spectra of device in transparent (red), black (blue), and mirror states (green). (b) Reflectance spectra of device in transparent (red), black (blue), and mirror states (green).

3.3 Study of cycling stability of the dip- and spin- coated devices

When an electrochromic device is repeatedly switched between its coloration and bleached states for a certain number of times, device failure occurs due to various faults and side reactions, such as electrode failure, electrolyte depravation, decay of active layer etc. Cycling stability of dip-coated and spin-coated electrodeposition-based electrochromic devices were investigated by repeatedly applying sequential voltages [28, 31, 46]. For the evaluation of device cycling stability, transmittance at 700 nm of dip-coated device in the transparent and black states was measured every 500 cycles. As shown in Figure 3a, the transmittance in transparent state is decreased and the transmittance in black state is slightly increased with the increase of cycles, with more cycles leading to poorer stability, as reported by previous literatures [28, 31, 46]. The change in optical transmittance contrast is measured to be 28% after 1500 cycles, indicating satisfactory device cycling stability. The cycling stability for

spin-coated device was also investigated by recording the optical transmittance contrast at every 500 cycles (Figure 3b). Sharply dropped transmittance contrast is exhibited with more cycles, with optical transmittance contrast of 16.4%, decrease in optical transmittance contrast of 66% obtained after 1500 cycles, indicating poorer cycling stability compared with that of the dip-coated device. The comparative study of dip and spin coated TiO_2 thin films reveals that the electrochromic properties can be strongly influenced by the film preparation method as aforementioned [38, 39].

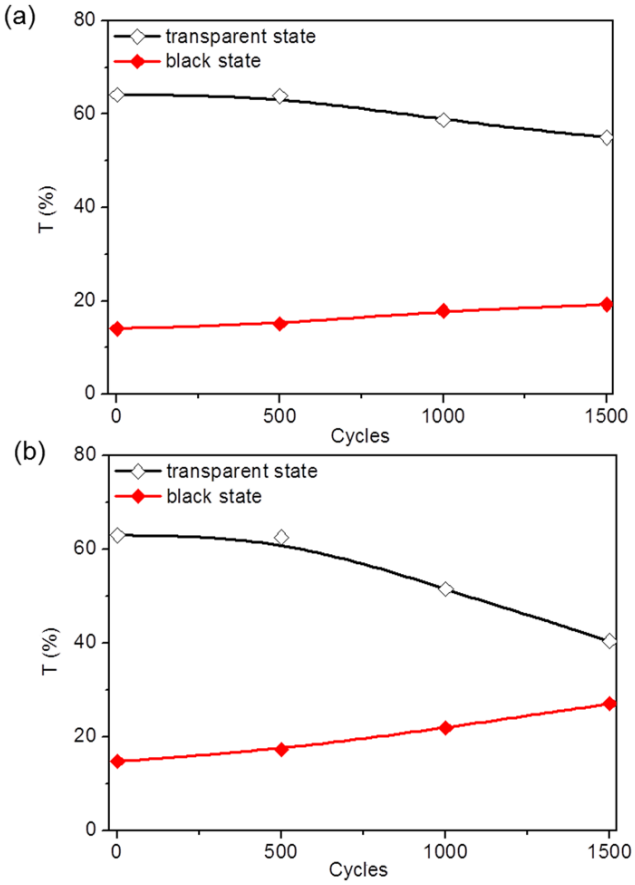

Figure 3. Transmittance variation for dip-coated device (a) and spin-coated device in transparent (black) and black (red) states at 700 nm after applying a sequence of voltages in the following order: -2.5 V (10 s), 0.5 V (30 s), 2.5 V (10 s), 0.5 V (20 s), with each of the 500 cycles was taken as a measurement node.

3.4 Structural features of the dip- and spin- coated TiO_2 thin films

The improved cycling stability of three-state electrochromic devices by modifying the electrode surface using dip-coating compared with that using spin-coating technique promote us to have a closer investigation on the structural and morphological features of the coated TiO_2 thin films. XRD patterns of sintered dip-coated TiO_2 film, sintered spin-coated TiO_2 film, and fresh TiO_2 nanoparticles without further treatment are recorded in the 2θ range from 20° to 80° [31, 47]. As presented in Figure 4, the diffraction peaks of two sintered TiO_2 films occur at the same positions and match very well with anatase structural form of TiO_2 (TiO_2 anatase, JCPDS 21-1217). These values are in good agreement

with literature data [47], with widened dispersion peaks appear in correspondence with crystal plane (101), (004), (200), (105), (211) and (204) of anatase phase. The observed extra peaks at 52° and 62° come from the FTO electrode surface, which matches well with the structural form of tin oxide (SnO_2, JCPDS 46-1088) [31, 48]. It can be seen that both the dip-coated and spin-coated TiO_2 thin films remain the same structural form as fresh TiO_2 nanoparticles throughout the whole fabricating procedure for modifying FTO electrode, indicating that the structural features of the coated TiO_2 thin films will not be influenced by the dip-coating and spin-coating methods, with similar results also presented by our previous report [31]. Hence, it is not the structural features of the dip and spin coated TiO_2 thin films that should be responsible for the enhanced cycling stability of dip-coated device.

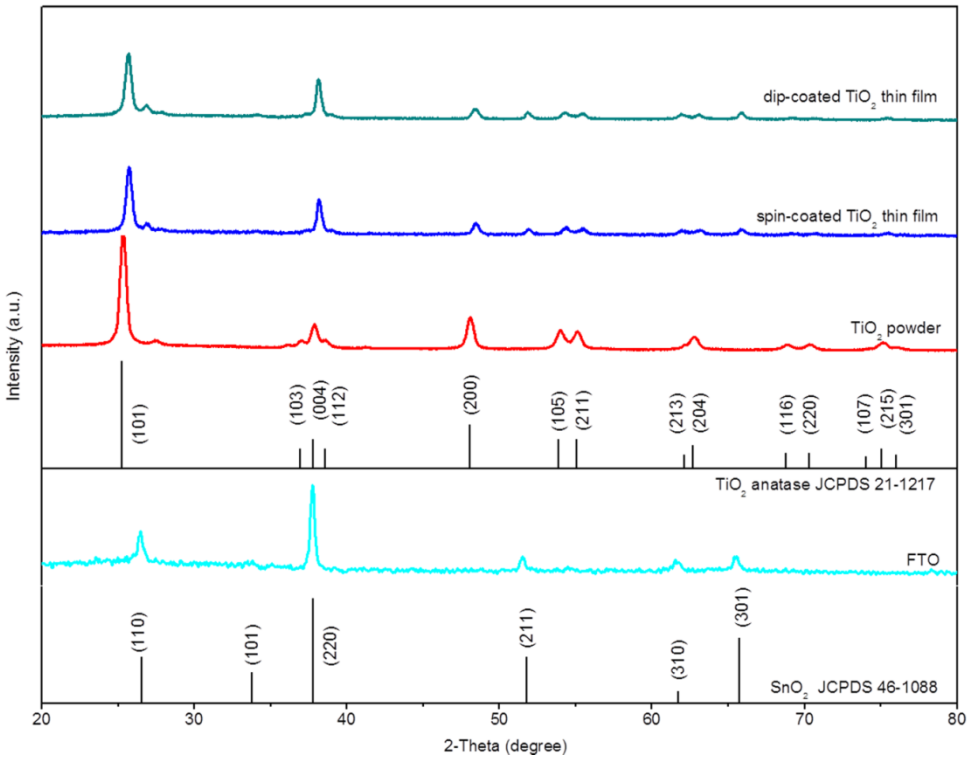

Figure 4. XRD patterns of dip-coated TiO_2 thin film (dip-coated on the FTO electrode and sintered at 500 °C for 30 min), spin-coated TiO_2 thin film (spin-coated on the FTO electrode and sintered at 500 °C for 30 min), fresh TiO_2 nanoparticles (purchased and untreated), flat FTO electrode (cleaned and dried).

3.5 Morphological features of the dip- and spin- coated TiO_2 thin films before and after 1500 cycles

The SEM micrographs at different magnifications of the dip-coated and spin-coated TiO_2 thin films before and after 1500 cycles are displayed in Figure 5 and Figure 7. The dip- and spin- coated TiO_2 thin films at lower magnification exhibit obvious difference in surface uniformity in terms of no oriented scratches observed for the dip-coated TiO_2 thin film (Figure 5a and 5b). Obvious difference in the morphological characteristics of the as-deposited spin- and dip- coated films at low magnifications are also observed for the WO_3 thin films, namely a crackfree morphology for the spin-coated film and dominant cracks for the spin-coated thin films [39]. Figure 5c presents a homogeneous surface morphology with a rough but not uneven surface of dip-coated TiO_2 thin film, which comprises dozens

of nanoparticles. The surface of the spin-coated TiO_2 thin film exhibits, however, non-uniform and large bumps, with local TiO_2 nanoparticles agglomeration and different sized pores inside displayed obviously, as illustrated in Figure 5d. Rough surfaces with nanoparticles agglomeration are also observed for the spin-coated ITO and TiO_2 nanoparticles onto transparent conductive electrodes [28-31]. It is thus can be seen that significant difference is exhibited for the surface topography of TiO_2 thin films deposited using spin-coating and dip-coating technique.

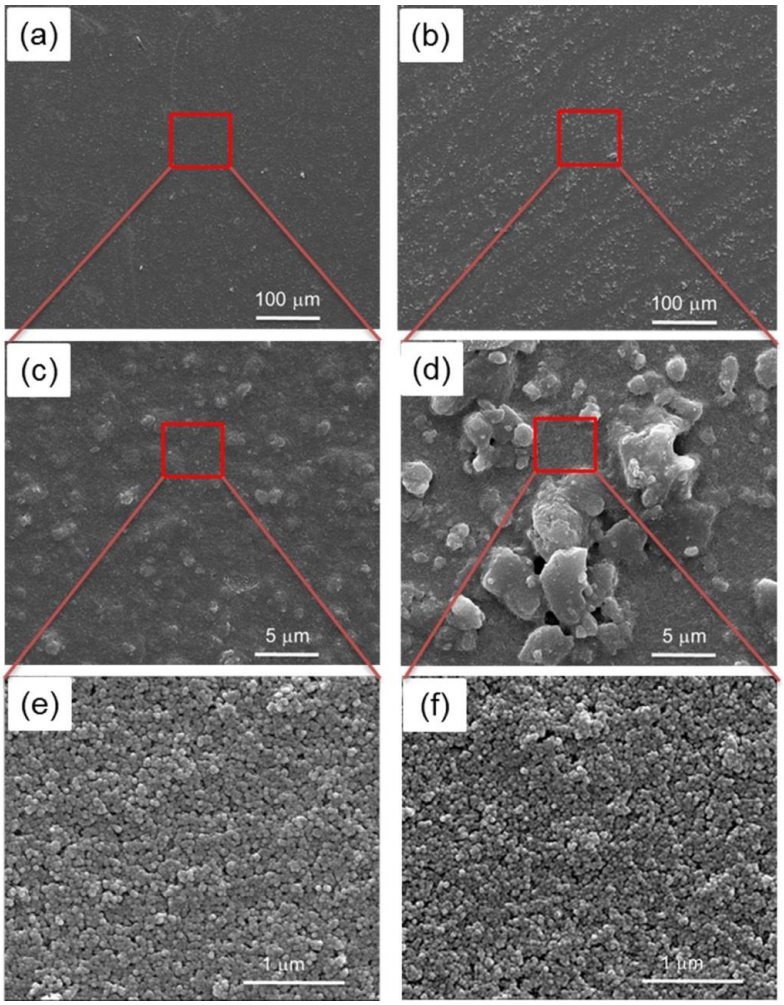

Figure 5. SEM images of dip-coated TiO_2 thin film at different magnifications (a, c, and e). SEM images of spin-coated TiO_2 thin film at different magnifications (b, d, and f).

The surface roughness of the dip-coated and spin-coated TiO_2 thin film were further measured by using an atomic force microscope (AFM), as shown in Figure 6a and 6b. Surface roughness is 42±15 nm for dip-coated TiO_2 thin film and 66±26 nm for spin-coated TiO_2 thin film, respectively, which are both smaller than the spin-coated ITO thin films [28] as a result of different nanoparticles size and modifying technique. The smaller fluctuation in average roughness value indicates a smoother and more uniform surface for the dip-coated TiO_2 thin film, as proved by the SEM images of dip-

coated TiO_2 thin film in Figure 5a. Thus, the fabrication method is crucial for uniform surface morphology of the TiO_2 thin film, which is an important factor for the cycling stability.

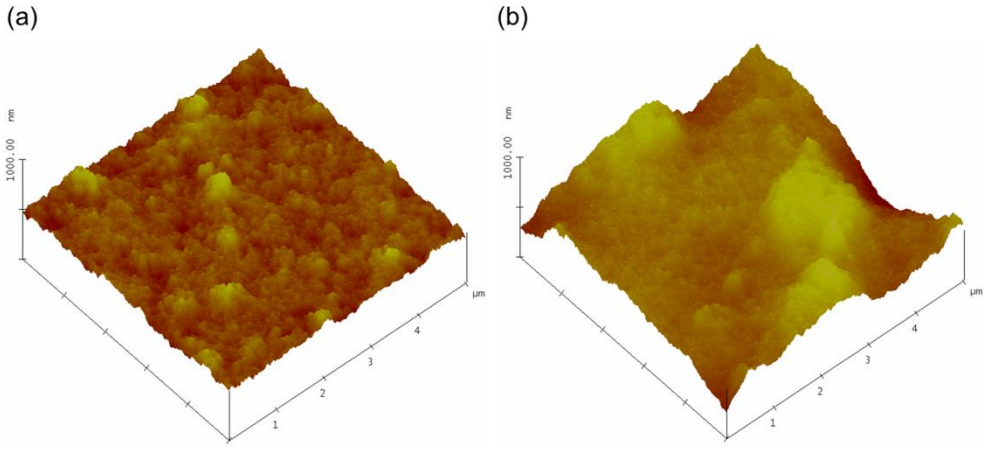

Figure 6. AFM image of dip-coated TiO_2 thin film (a); AFM image of spin-coated TiO_2 thin film (b).

Generally, in comparison with compact thin films, the rough thin films offer potential advantages in the electrochromic device due to their large active surface area that could increase the efficient contact area between the electrode and the electrolyte [49]. Although, the larger active surface area of TiO_2 thin film obtained by spin-coating has the ability to accelerate the Ag deposition onto FTO electrode, the Ag dissolution back into electrolyte is, however, slowed down. The obstructed Ag dissolution caused by large active surface area might be further proved by the longer switching time for device transforms from coloration to transparent state compared with their opposite process [31]. The nanoparticles agglomeration onto the surface of modified FTO electrode hinders the Ag leave the rough surface easily, leading to a poor cycling stability of the electrodeposition-based electrochromic device. The surfaces of both the dip-coated and spin-coated TiO_2 thin films exhibit homogeneous and fined-grained surface for their smooth regions, with sharp and well-defined boundaries between grains as well as a uniform distribution of pores and grains observed (Figure 5e and 5f). The homogeneous and fined-grained surface for the smooth regions at higher magnification are in agreement with reported values for spin-coated ITO and TiO_2 thin films [28, 31]. Although the difference in the surface roughness for smooth regions is quite modest, the improved uniformity of the dip-coated TiO_2 thin film surface is conducive to the enhancement of the cycling stability as a result of less segregation of electrolytes and quick dissolution of Ag back into electrolyte during the switching between the coloration and bleaching states.

Furthermore, the morphological features of the dip and spin coated TiO_2 thin films after manifold cycles were investigated. As shown in Figure 7a and 7b, uneven electrolyte agglomeration is observed for both the dip and spin coated TiO_2 thin films. As previous reported [46, 50, 51], loose surface with irregular cracks, emerging nanoparticles or erosion and self dissolution of surface layer can be seen for thin films after long time cycling. We supposed that the ability to achieve complete reversibility is deteriorated due to the gradual deposition of Ag onto bumps of TiO_2 thin films and

inability to dissolve Ag back into electrolyte immediately during the continuous cycling between the coloration and bleaching states. Moreover, the electrolyte agglomeration is more obvious for spin-coated TiO_2 thin film after 1500 cycles. It is thus can be seen that the non-uniform deposition of electrolyte onto the TiO_2 thin film results in the device failure, with more TiO_2 nanoparticles agglomeration leading to poorer cycling stability. Therefore, the difference in surface uniformity and roughness of dip-coated and spin-coated TiO_2 thin films might be the main factors to influence the device optical contrast and cycling stability.

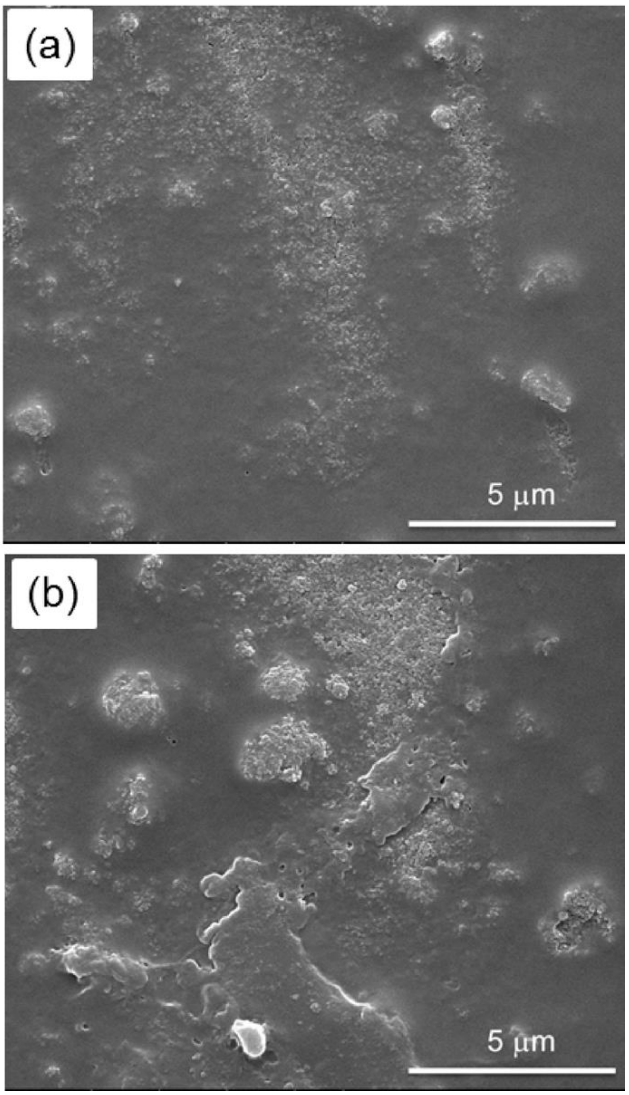

Figure 7. SEM images of dip-coated (a) and spin-coated (b) TiO_2 thin film after switching between its coloration and bleached states for 1500 cycles

4. CONCLUSIONS

In summary, we have revealed an easy-to-apply and well-controlled dip-coating technique to deposit TiO_2 nanoparticles on FTO electrodes for the first time. The electrodeposition-based electrochromic devices are fabricated, achieving voltage-controlled, reversible, three optical states

transformation, namely, the mirror, transparent, and black states. The dip-coated device has a high optical contrast with transmittance below 1% in the black state and reflectance over 70% in the mirror state. Moreover, the dip-coated device shows satisfactory cycling stability, with decrease in optical transmittance contrast of 28% after 1500 cycles, better than that of spin-coated devices because of the dip-coated smooth and uniform TiO_2 thin film. The obvious difference of morphological features between the dip- and spin-coated TiO_2 thin films reveals the relevance between the modifying film preparation method and device electrochromic properties, and illustrates the huge influence of thin films overall surface roughness to the cycling stability of electrodeposition-based electrochromic device. The mechanism of the inability for the fabricated electrochromic devices to achieve complete reversibility after long time cycling is also discussed in this paper. Screening and fabricating electrodeposition-based electrochromic device with optimal electrochromic properties by manipulating dip-coated parameters is ongoing. The TiO_2 nanoparticle-modified device with reversible three-state optical transformation may have various applications, such as information displays and light-modulation devices.

ACKNOWLEDGEMENTS
The authors acknowledge the financial support from National Natural Science Foundation of China [Grant #: 51472044].

References

1. S. K. Deb, *Appl. Optics,* 8 (1969) 192.
2. C. Bechinger, S. Ferrer, A. Zaban, J. Sprague and B. A. Gregg, *Nature,* 383 (1996) 608.
3. U. Bach, D. Corr, D. Lupo, F. Pichot and M. Ryan, *Adv. Mater.,* 14 (2002) 845.
4. S. I. Cho, W. J. Kwon, S. J. Choi, P. Kim, S. A. Park, J. Kim, S. J. Son, R. Xiao, S. H. Kim and S. B. Lee, *Adv. Mater.,* 17 (2005) 171.
5. A. Kraft and M. Rottmann, *Sol. Energ. Mat. Sol. C.,* 93 (2009) 2088.
6. M. P. Browne, H. Nolan, N. C. Berner, G. S. Duesberg, P. E. Colavita and M. E. G. Lyons, *Int. J. Electrochem. Sc.,* 11 (2016) 6636.
7. F. C. Krebs, *Nature Mater.,* 7 (2008) 766.
8. P. M. S. Monk, C. Turner and S. P. Akhtar, *Electrochim. Acta,* 44 (1999) 4817.
9. B. T. Sone, S. N. Mailu, T. Malwela, E. Coetsee, H. C. Swart, E. I. Iwuoha and M. Maaza, *Int. J. Electrochem. Sc.,* 9 (2014) 2867.
10. G. A. Niklasson and C. G. Granqvist, *J. Mater. Chem.,* 17 (2007) 127.
11. D. M. DeLongchamp and P. T. Hammond, *Adv. Funct. Mater.,* 14 (2004) 224.
12. K. Itaya, I. Uchida and V. D. Neff, *Acc. Chem. Res.,* 19 (1986) 162.
13. K. Lin, S. Zhang, H. Liu, Y. Zhao, Z. Wang and J. Xu, *Int. J. Electrochem. Sc.,* 10 (2015) 7720.
14. W. Lu, A. G. Fadeev, B. H. Qi, E. Smela, B. R. Mattes, J. Ding, G. M. Spinks, J. Mazurkiewicz, D. Z. Zhou, G. G. Wallace, D. R. MacFarlane, S. A. Forsyth and M. Forsyth, *Science,* 297 (2002) 983.
15. T. Kakibe and H. Ohno, *J. Mater. Chem.,* 19 (2009) 4960.
16. X. W. Sun and J. X. Wang, *Nano Lett.,* 8 (2008) 1884.
17. G. de la Torre, C. G. Claessens and T. Torres, *Chem. Commun.,* (2007) 2000.
18. Q. Zeng, A. McNally, T. E. Keyes and R. J. Forster, *Electrochem. Commun.,* 10 (2008) 466.

19. H. Ling, J. Lu, S. Phua, H. Liu, L. Liu, Y. Huang, D. Mandler, P. S. Lee and X. Lu, *Journal of Materials Chemistry A*, 2 (2014) 2708.
20. S. Xiong, S. L. Phua, B. S. Dunn, J. Ma and X. Lu, *Chem. Mater.*, 22 (2010) 255.
21. C. O. Avellaneda, M. A. Napolitano, E. K. Kaibara and L. O. S. Bulhoes, *Electrochim. Acta*, 50 (2005) 1317.
22. S. I. C. deTorresi and I. A. Carlos, *J. Electroanal. Chem.*, 414 (1996) 11.
23. A. Imamura, M. Kimura, T. Kon, S. Sunohara and N. Kobayashi, *Sol. Energ. Mat. Sol. C.*, 93 (2009) 2079.
24. M. Nakashima, T. Ebine, M. Shishikura, K. Hoshino, K. Kawai and K. Hatsusaka, *ACS Appl. Mater. Interfaces*, 2 (2010) 1471.
25. M. R. S. Oliveira, D. A. A. Mello, E. A. Ponzio and S. C. de Oliveira, *Electrochim. Acta*, 55 (2010) 3756.
26. J. P. Ziegler and B. M. Howard, *Sol. Energ. Mat. Sol. C.*, 39 (1995) 317.
27. J. P. Ziegler, *Sol. Energ. Mat. Sol. C.*, 56 (1999) 477.
28. S. Araki, K. Nakamura, K. Kobayashi, A. Tsuboi and N. Kobayashi, *Adv. Mater.*, 24 (2012) OP122.
29. A. Tsuboi, K. Nakamura and N. Kobayashi, *J. Soc. Inf. Display*, 21 (2013) 361.
30. A. Tsuboi, K. Nakamura and N. Kobayashi, *Adv. Mater.*, 25 (2013) 3197.
31. T. Ye, Y. Xiang, H. Ji, C. Hu and G. Wu, *RSC Adv.*, 6 (2016) 30769.
32. H. C. Chen, D. J. Jan, Y. S. Luo and K. T. Huang, *Appl. Optics*, 53 (2014) A321.
33. B. Reichman and A. J. Bard, *J. Electrochem. Soc.*, 126 (1979) 583.
34. T. Maruyama and S. Arai, *Sol. Energ. Mat. Sol. C.*, 30 (1993) 257.
35. S.-I. Park, Y.-J. Quan, S.-H. Kim, H. Kim, S. Kim, D.-M. Chun, C. S. Lee, M. Taya, W.-S. Chu and S.-H. Ahn, *Int. J. Pr. Eng. Man.-G. T.*, 3 (2016) 397.
36. J. Livage and D. Ganguli, *Sol. Energ. Mat. Sol. C.*, 68 (2001) 365.
37. Z. C. Wang and X. F. Hu, *Thin Solid Films*, 352 (1999) 62.
38. M. Deepa, R. Sharma, A. Basu and S. A. Agnihotry, *Electrochim. Acta*, 50 (2005) 3545.
39. M. Deepa, T. K. Saxena, D. P. Singh, K. N. Sood and S. A. Agnihotry, *Electrochim. Acta*, 51 (2006) 1974.
40. C. Park, S. Seo, H. Shin, B. D. Sarwade, J. Na and E. Kim, *Chem. Sci.*, 6 (2015) 596.
41. B. G. Xie, J. J. Sun, Z. B. Lin and G. Nan. Chen, *J. Electrochem. Soc.*,156 (2009) D79.
42. T.-Y. Kim, S. M. Cho, C. S. Ah, K. -S. Suh, H. Ryu and H. Y. Chu, J. Inf. Display, 15 (2014) 13.
43. B. Laik, D. Carrie`re and J. -M. Tarascon, *Electrochim. Acta*, 46 (2001) 2203.
44. Z. M. He, X. Yuan, Q. Wang, L. Yu, C. Zou, C. Y. Li, Y. Z. Zhao, B. F. He, L. Y. Zhang, H. Q. Zhang and H. Yang, *Adv. Optical Mater.*, 4 (2016) 106.
45. K. Shinozaki, SID Digest, 33 (2002) 39.
46. J. L. Zhou, G. Luo, Y. X. Wei, J. M. Zheng and C. Y. Xu, *Electrochim. Acta*, 186 (2015) 182.
47. W. Niu, G. Wang, X. D. Liu, J. Tang and X. G. Bi, *Int. J. Electrochem. Sc.*, 10 (2015) 2613.
48. D. D. Yao, R. A. Rani, A. P. O'Mullane, K. K.-Zadeh and J. Zhen. Ou, *J. Phys. Chem. C*, 118 (2014) 10867.
49. R. Viennet, J. P. Randin, I. D. Raistrick, *J. Electrochem. Soc.*, 129 (1982) 2451.
50. Y. Ren, W.K. Chim, L. Guo, H. Tanoto, J.S. Pan and S.Y. Chiam, *Sol. Energ. Mat. Sol. C.*, 116 (2013) 83.
51. K. Huang, J. F. Jia, Q. T. Pan, F. Yang and D. Y. He, *Physica B*, 396 (2007) 164.